J. metamorphic Geol., 2003, **21,** 723–735

Lawsonite growth in the epidote blueschists from the Ile de Groix (Armorican Massif, France): a potential geobarometer

M. BALLEVRE,[1] P. PITRA[1] AND M. BOHN[2]
[1]*Equipe Lithosphère, Géosciences Rennes (UMR-CNRS 6112), Université de Rennes I, F-35042 Rennes CEDEX, France (Michel.Ballevre@Univ-rennes1.fr)*
[2]*Microsonde Ouest, IFREMER and CNRS, Centre de Brest, BP 70, F-29280 Plouzané, France*

ABSTRACT The garnet blueschists from the Ile de Groix (Armorican Massif, France) contain millimetre- to centimetre-sized pseudomorphs consisting of an aggregate of chlorite, epidote and paragonite. The pseudomorphed phase developed at a late stage of the deformation history, because it overgrows a glaucophane–epidote–titanite foliation. Garnet growth occurred earlier than the beginning of the ductile deformation, and thus garnet is also included in the pseudomorphs. Microprobe analyses show that garnet is strongly zoned, with decreasing spessartine and increasing almandine and pyrope contents from core to rim. Grossular content is higher in garnet cores (about 35 mole%) compared to garnet rims (about 30 mole%). Blue amphibole has glaucophane compositions with a low Fe^{3+} content and become more magnesian when inclusions in garnet ($X_{Mg} = 0.62$–0.65) are compared with matrix grains ($X_{Mg} = 0.67$–0.70). Matrix epidote has a pistacite content of about 50 mole%. On the basis of their shape and the nature of the breakdown products, the pseudomorphs are attributed to lawsonite. A numerical model (using THERMOCALC) has been developed in order to understand the reactions controlling both the growth and the breakdown of lawsonite. Lawsonite growth could have taken place through the continuous hydration reaction Chl + Ep + Pg + Qtz + Vap = Gln + Lws, followed by the fluid-absent reaction Chl + Ep + Pg = Grt + Gln + Lws. Peak *P*–*T* conditions are estimated at about 18–20 kbar, 450 °C. This indicates that lawsonite growth took place at increasing *P* and *T*, hence can be used as a geobarometer in the buffering assemblage garnet–glaucophane–epidote. The final part of the history is recorded by lawsonite breakdown, after cessation of the ductile deformation, and recording the earliest stages of the exhumation.

Key words: Armorican Massif; blueschist; Ile de Groix; lawsonite pseudomorph; *P*–*T* history.

INTRODUCTION

Lawsonite ($CaAl_2Si_2O_7(OH)_2.H_2O$) is an orthorhombic sorosilicate with high H_2O content (about 12 wt%). Lawsonite is reported in most blueschist facies rocks world-wide (e.g. Van der Plas, 1959; Deer *et al*., 1986; with references therein). The lawsonite stability field has been experimentally determined over a large range of *P*–*T*–*X*(CO_2) conditions (Newton & Kennedy, 1963; Nitsch, 1972; Chatterjee *et al*., 1984; Heinrich & Althaus, 1988). Because lawsonite is potentially a major source of water in subducting oceanic crust, experimental data have been more recently extended to ultra-high pressures in synthetic (Pawley, 1994; Schmidt & Poli, 1994; Schmidt, 1995; Poli & Schmidt, 1998; Grevel *et al*., 2001) as well as natural (in most cases MORB + H_2O) systems (Domanik & Holloway, 1996; Liu *et al*., 1996; Ono, 1998; Okamoto & Maruyama, 1999). Finally, calculated petrogenetic grids for a variety of sodic amphibole compositions (Evans, 1990) indicate that glaucophane-lawsonite is a lower temperature association compared to glaucophane-epidote.

Lawsonite pseudomorphs are frequently reported from most blueschist belts, like the Alpine belt (e.g. Ellenberger, 1960; Fry & Fyfe, 1971; Bearth, 1973; Fry, 1973; Höck, 1974; Caron, 1977; Sicard *et al*., 1984; Martin & Tartarotti, 1989; Cannic *et al*., 1996), the Aegean belt (Dixon, 1969, 1976; Okrusch *et al*., 1978; Will *et al*., 1998), as well as in Alaskan (Forbes *et al*., 1984; Thurston, 1985; Patrick & Evans, 1989) and Caribbean (Green *et al*., 1968) blueschists. Lawsonite pseudomorphs have also been identified in Palaeozoic blueschists, like the Uralian belt (Maksyutovo Complex: Dobretsov *et al*., 1974; Schulte & Sindern, 2002) and the Variscan belt (Ile de Groix: Cogné *et al*., 1966; Felix & Fransolet, 1972). Although pseudomorphs are not isochemical, lawsonite is identified because of its square to lozenge shape and its breakdown products, involving in most cases epidote and paragonite.

Two general solutions have been proposed for explaining lawsonite pseudomorphs in terms of the *P*–*T* evolution of the blueschists. First, lawsonite could have grown in a rock devoid of epidote, recording an earlier, prograde, stage. Lawsonite breakdown could thus result from an increase in pressure and/or temperature, leading to epidote-bearing blueschists (e.g. Martin & Tartarotti, 1989), or a decrease in pressure at the beginning of their exhumation history (e.g. Will

et al., 1998). Second, lawsonite growth could occur in an epidote-bearing blueschist because of a decrease in temperature during the earliest stage of decompression, followed by its breakdown during isothermal decompression (Barnicoat & Fry, 1986; Fry & Barnicoat, 1987). This paper will show that none of the above proposals can be applied to the Ile de Groix blueschists, where lawsonite growth took place at increasing pressure in an epidote-bearing blueschist.

GEOLOGICAL SETTING

The studied samples have been collected in the Ile de Groix, a small island off the southern coast of Brittany (France), well known for its beautifully preserved blueschists (Barrois, 1883; Makanjuola & Howie, 1972; Triboulet, 1974; Carpenter, 1976; Barrientos, 1992; Audren *et al.*, 1993). The island shows interlayered metapelites and metabasites, the latter being either small (1–5 m) lenses (boudinaged layers or isoclinal, rootless folds) or thick layers (up to a few dozen metres). Interlayering of micaschists and blueschists is observed at varying scales, with minor layers no less than a few centimetres in thickness. Amongst the metabasites, blueschists are largely predominant in the eastern part of the island, whereas greenschists predominate in the western part of the island (Triboulet, 1974; Carpenter, 1976; Audren *et al.*, 1993). The blueschist facies metamorphism is associated with an intense ductile deformation, interpreted either as recording the northwards obduction of a piece of oceanic lithosphere (Quinquis & Choukroune, 1981) or vertical shortening during crustal extension (Shelley & Bossière, 1999).

Mineral assemblages in the metabasites are indicative of a spatial zonation of the blueschist facies metamorphism (Triboulet, 1974; Carpenter, 1976) with higher-grade, garnet-bearing, assemblages in the eastern part of the island (Fig. 1). The garnet isograd has been recently re-interpreted as a ductile thrust, the higher-grade (eastern) unit being thrust over the lower-grade (western) unit (Bosse *et al.*, 2002). In the eastern part of the island, some blueschists display abundant lozenge-shaped pseudomorphs attributed to lawsonite (Cogné *et al.*, 1966; Felix, 1972a,b; Felix & Fransolet, 1972). Meanwhile, the identification of lawsonite has been cast in doubt for three main reasons: (i) no relics of fresh lawsonite have ever been found; (ii) estimated P–T conditions for the blueschist facies metamorphism in the Ile de Groix are outside the experimentally determined stability field for lawsonite (Audren & Triboulet, 1984; Djro *et al.*, 1989); (iii) calcium-bearing plagioclase (such as oligoclase or andesine) rather than lawsonite is a valid candidate for the pseudomorphed mineral (Shelley & Bossière, 1999). This paper attempts to solve the problem, and aims to show that the pseudomorphs derive from lawsonite. Additionally, an unexpected result from this study is the identification of the lawsonite-producing reaction, which provides a potential geobarometer and helps clarifying the P–T path of the blueschists.

Careful examination of the mafic blueschists from the Ile de Groix reveals that rectangular to lozenge-shaped pseudomorphs are not distributed evenly through the island (Fig. 1). The pseudomorphs are abundant in the blueschists from the eastern part of the island (Felix, 1972b), i.e. in the Upper Unit, where they are found in layers up to 1 m thick as well as in isolated mafic lenses. Two main types of rocks are recognised. Some pale-coloured blueschists display abundant centimetre-sized pseudomorphs (Fig. 2) in a matrix essentially consisting of glaucophane, epidote and minute ($<$ 1 mm) garnet grains, the latter being also present within the pseudomorphs. In dark-coloured blueschists, the pseudomorphs are set in a matrix of blue-black glaucophane, yellow epidote and large (2–5 mm) garnet grains, the latter being rarely partially enclosed within the pseudomorphs. Some pseudomorphs with similar shapes are also found in a garnet–epidote micaschist belonging to the Upper Unit. The pseudomorphs are lacking in the western part of the island, i.e. in the Lower Unit, except in rare lenses of Fe-glaucophane-ankerite-epidote mafic schists (Baie des Curés: Carpenter, 1976; Bernard-Griffiths *et al.*, 1986; vallon de Storang), which are out of the scope of this paper.

TEXTURAL RELATIONSHIPS

Most pseudomorph-bearing samples are similar in terms of microstructural development (Felix, 1972b), although large variations in the modal proportions of the breakdown products in the pseudomorphs are found. Sample TRE 1 has been chosen for a detailed study because its microstructural history is unambiguous, allowing precise timing of the growth of most phases, including the pseudomorphed mineral (Fig. 3).

Sample TRE 1 is a pale-coloured, fine-grained blueschist, where the foliation is defined by glaucophane, epidote and titanite. Idioblastic

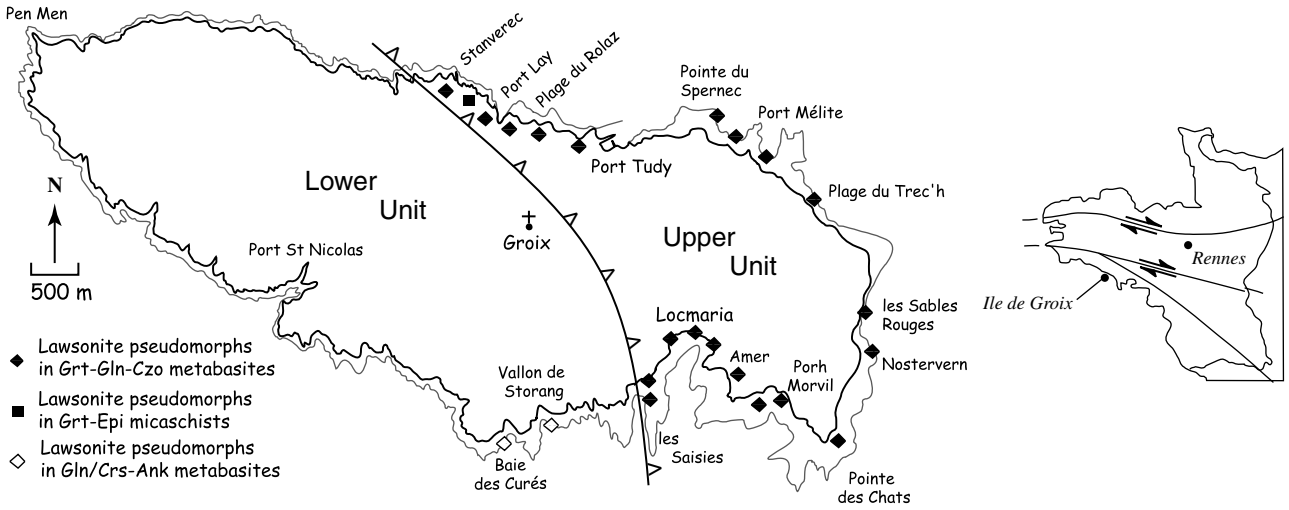

Fig. 1. Distribution of lawsonite pseudomorphs in the Ile de Groix. This map is a compilation of data from Felix (1972b), Carpenter (1976), Pierrot *et al.* (1980), and Bernard-Griffiths *et al.* (1986) and field observations by M. Ballèvre and V. Bosse. A higher-grade Upper Unit, where the assemblage Mn-poor garnet-chloritoid-glaucophane defines peak P–T conditions, is thrust over a lower grade unit, characterized by chloritoid-chlorite ($\pm$ Mn-rich garnet) in the metapelites (Bosse *et al.*, 2002). Note that lawsonite pseudomorphs in the garnet–epidote blueschists are found only in the Upper Unit. Inset shows the location of the island in the Armorican massif (western France).

Fig. 2. Lawsonite pseudomorphs in a garnet-bearing blueschist from the Ile de Groix. The photograph shows a weathered outcrop on the southern coast of the island (Amer on Fig. 1). In this locality, the pseudomorphs stand out of the rock, and can be hand-picked for measuring the interfacial angles (Felix & Fransolet, 1972).

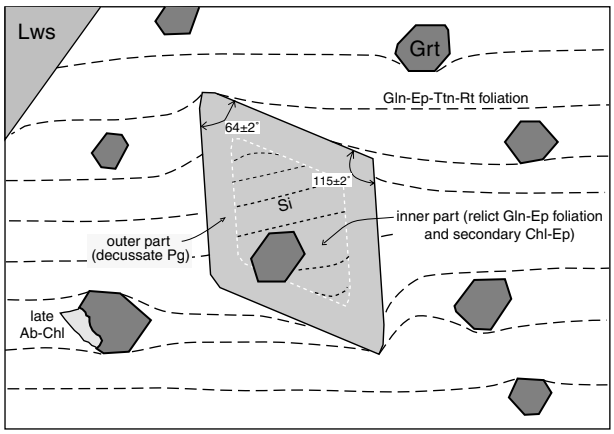

Fig. 3. Microstructure of sample TRE 1 (Trech on Fig. 1). Interfacial angles of the pseudomorphs are taken from Felix & Fransolet (1972). The pseudomorphed phase overgrew a foliated matrix consisting of epidote-glaucophane-titanite. Relics of this earlier schistosity are mainly found in the core of the pseudomorphs, which is consistent with the abundance and distribution of the inclusions in fresh as well as pseudomorphed lawsonite in other localities (e.g. Caron, 1977; Compagnoni, 1977; Pognante, 1989).

garnet grains (0.5–1 mm in diameter) are dispersed in the glaucophane matrix. Conspicuous lozenge-shaped white aggregates (up to 2 cm in their longest dimension) are also irregularly dispersed in the rock, and they do not show a preferential shape orientation (Fig. 2). The glaucophane foliation wraps around the pseudomorphs, indicating that some ductile deformation took place during or after the growth of the pseudomorphed porphyroblast. The pseudomorphs consist of an aggregate of white mica, chlorite and epidote, with some quartz present in a few pseudomorphs. As noted by Felix (1972b), epidote is mainly concentrated in the core of the pseudomorphs while white mica is preferentially distributed along the margins of the pseudomorphs. Other phases in the pseudomorphs are glaucophane, crystals of which are mainly concentrated in the core of the pseudomorphs, garnet and titanite. Glaucophane crystals and some of the epidote grains are aligned parallel to each other, and define an internal schistosity, interpreted as a relict foliation that has been overgrown by the pseudomorphed porphyroblasts. This interpretation, already stressed by Felix (1972a,b), indicates that the porphyroblasts grew in a foliated matrix consisting of glaucophane, epidote and garnet.

Matrix garnet shows inclusions of epidote, actinolite, glaucophane, abundant titanite and minor rutile with some quartz and apatite. Core inclusions are not aligned (i.e. they do not define a relic, included, schistosity), but rim inclusions tend to be parallel to the matrix foliation, suggesting foliation development at a late stage of garnet growth (Fig. 3). Further indication in favour of a late foliation development during garnet growth is provided by the titanite aggregates, which display irregular shapes in garnet cores, then become flattened towards the garnet rims, and are continuous with the alignment of titanite grains defining the matrix foliation. In short, garnet growth began before and continued during ductile deformation, while the growth of the pseudomorphed mineral took place during ductile deformation.

Three types of post-kinematic, retrograde, transformations are identified. First, the breakdown products in the pseudomorphs are not oriented. Second, some glaucophane grains are epitactically overgrown by a dark-coloured, blue-green, amphibole. Third, a few garnet grains are partially replaced by chlorite–albite aggregates, which could constitute small pressure shadows around garnet. In this case, garnet faces are not regular, but convex towards the garnet core, clearly implying late garnet dissolution.

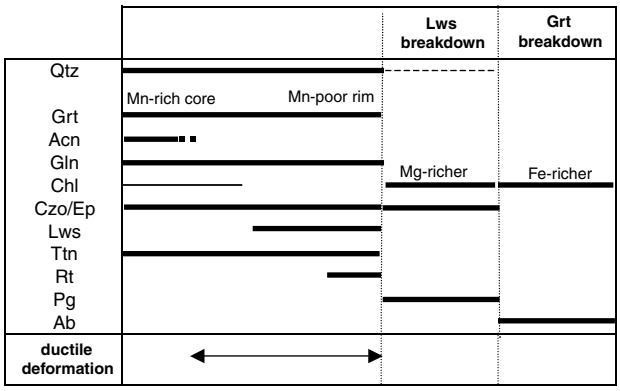

Fig. 4. Relationships between mineral growth and ductile deformation in sample TRE 1. The presence of chlorite in the earlier stage of garnet growth is assumed because of the occurrence of a single chlorite in a garnet core, although it is not entirely clear if this chlorite occurs in a late, narrow, fracture, or was trapped during garnet growth. Ductile deformation took place during growth of the pseudomorphosed phase, and ceased when this phase broke down.

Table 1. Representative analyses of coexisting minerals in sample TRE 1.

	Inclusion assemblage					Matrix assemblage				Pseudomorph			Grt/Gln	
Mineral	Grt core	Gln	Acn	Czo	Ttn	Grt rim	Gln	Czo	Ttn	Czo	Chl	Pg	Chl	Ab
Analysis	4	66	28	13	16	5	59	26	23	78	76	71	62	60
SiO_2	37.30	57.33	56.21	38.48	30.18	37.59	58.45	38.46	30.52	38.32	27.16	47.04	27.55	68.59
TiO_2	0.17	0.02	0.02	0.22	38.16	0.03	0.00	0.12	38.64	0.06	0.10	0.03	0.01	0.00
Al_2O_3	21.00	11.22	1.84	27.43	2.30	21.31	11.38	26.94	1.59	27.68	20.18	39.50	19.88	19.35
Cr_2O_3	0.03	0.01	0.00	0.00	0.08	0.00	0.11	0.05	0.00	0.00	0.08	0.07	0.07	0.00
FeO	18.69	11.12	9.65	6.67	0.77	27.75	9.39	7.47	0.37	6.65	20.57	0.26	22.59	0.29
MnO	10.31	0.16	0.54	0.62	0.07	0.64	0.02	0.02	0.04	0.44	0.13	0.01	0.14	0.00
MgO	0.76	9.72	17.62	0.02	0.01	2.30	10.44	0.06	0.00	0.03	18.65	0.25	16.46	0.00
CaO	12.17	0.95	11.42	23.50	28.33	10.59	0.65	24.04	28.81	23.80	0.08	0.14	0.07	0.42
Na_2O	0.02	6.69	1.10	0.00	0.04	0.01	6.64	0.00	0.01	0.02	0.03	7.16	0.07	11.59
K_2O	0.00	0.02	0.02	0.00	0.00	0.00	0.00	0.00	0.00	0.00	0.02	0.82	0.23	0.05
Total	100.45	97.24	98.42	96.94	99.94	100.21	97.06	97.16	99.98	97.00	87.00	95.28	87.07	100.29
Cations on the basis of	*	**	**	12.5 O	5 O	*	**	12.5 O	5 O	12.5 O	36 O	22 O	36 O	8 O
Si	2.96	7.94	7.87	3.01	0.99	2.97	7.97	3.00	1.00	3.00	5.61	6.01	5.75	2.99
Ti	0.01	0.00	0.00	0.01	0.94	0.00	0.00	0.01	0.95	0.00	0.02	0.00	0.00	0.00
Al	1.97	1.83	0.30	2.53	0.09	1.98	1.89	2.48	0.06	2.55	4.91	5.95	4.89	0.99
Cr	0.00	0.00	0.00	0.00	0.00	0.00	0.00	0.00	0.00	0.00	0.01	0.01	0.01	0.00
Fe^{3+}	0.09	0.06	0.16	0.44		0.07	0.03	0.49		0.43				
Fe^{2+}	1.15	1.22	0.97		0.02	1.76	1.01		0.00	3.56	0.03	3.94	0.01	
Mn	0.69	0.02	0.06	0.04	0.00	0.04	0.01	0.00	0.00	0.03	0.02	0.00	0.03	0.00
Mg	0.09	2.00	3.67	0.00	0.00	0.27	2.15	0.01	0.00	0.00	5.75	0.05	5.12	0.00
Ca	1.03	0.14	1.71	1.97	0.99	0.90	0.07	2.01	1.01	1.99	0.02	0.02	0.02	0.02
Na	0.00	1.80	0.30	0.00	0.00	0.00	1.87	0.00	0.00	0.00	0.01	1.77	0.03	0.98
K	0.00	0.00	0.00	0.00	0.00	0.00	0.00	0.00	0.00	0.00	0.01	0.13	0.06	0.00
Total	8.00	15.02	15.05	8.00	3.03	8.00	15.00	8.00	3.02	8.01	19.91	13.97	19.84	5.00
XMg	0.05	0.62	0.78			0.13	0.68				0.62		0.56	
Alm	0.39					0.59								
Sps	0.23					0.01								
Prp	0.03					0.09								
Grs	0.35					0.30								

* Ferric iron in garnet is calculated on the basis of 12 oxygen and 8 cations.

** Ferric iron in amphibole is calculated according to Leake *et al.* (1997). The formula shown is the mean of the estimated minimum and maximum Fe^{3+} contents.

To sum up, the paragenetic history of sample TRE 1 (Fig. 4) is characterized by three stages, namely (i) garnet cores in equilibrium with actinolite, glaucophane, epidote and titanite (ii) garnet rims in equilibrium with glaucophane, epidote and the pseudomorphed phase, and (iii) breakdown of the pseudomorphed phase into chlorite-epidote-mica and chlorite-albite growth at the garnet–glaucophane interface. Ductile deformation began during garnet growth and ceased before stage (iii).

MINERAL CHEMISTRY

Microprobe analyses of minerals have been performed with a Cameca SX50 (Microsonde Ouest). Operating conditions for spot analyses were 20 kV accelerating voltage, 20 nA sample current and 20 s counting time. Representative spot analyses are given in Table 1. Particular attention has been paid to garnet zonation, by creating X-rays element maps for Fe, Mn, Mg and Ca (Fig. 5), and by analyzing a few detailed traverses across the zoned crystals (Fig. 6). Garnet is strongly zoned, with decreasing Sps (from about 20–25 mole% to 1–2 mole%) and increasing Alm and Prp contents, from core to rim (Table 1). The bell-shaped curve of Sps is well shown, as is the mirror image provided by Alm. The Grs content is less variable, but its amount is slightly lower towards the margin (about 30 mole%) compared to the core (about 35 mole%). The same zoning pattern is observed in matrix garnet grains or in grains partially or totally enclosed in the pseudomorphs. This type of zoning profile is typical of growth zoning.

Details of the growth history are suggested by the composition maps, explaining why the profile is asymmetric with respect to garnet core. Indeed, the compositional gradient is much steeper in the left part of the profile and smoother in the right part of the profile. During garnet growth, adjacent grains were either dissolved or included within garnet, depending whether they participated or did not participate in the continuous reaction controlling garnet growth. For example, minute titanite inclusions aligned in the north-western part of the imaged garnet provided an effective barrier to the advancement of the garnet face. The zoning pattern against the large glaucophane inclusion suggests that the amphibole also acted as a barrier during garnet growth. When the garnet face was growing against reactant minerals that were progressively dissolved, the chemical gradient is smoother (see right part of the zoning profile, and the corresponding part of the garnet image).

Microprobe analyses of amphibole have been recalculated according to the procedure outlined by J. Schumacher (in Leake *et al.*, 1997), and the following uses the average estimate for Fe^{3+}. Three types of amphiboles are distinguished. First, actinolite ($X_{Mg} = 0.76$–0.80) is only present as rare inclusions within the Sps-rich garnet cores. This actinolite is characterized by a relatively high Al_2O_3 and Na_2O contents (up to 3.5 and 1.25 wt%, respectively), which is consistent with its coexistence at relatively high pressures with glaucophane (Reynard & Ballèvre, 1987; Smelik & Veblen, 1992). Second, glaucophane is present as inclusions in garnet, both in the Sps-rich cores and in the Sps-poor rims, and is the dominant matrix amphibole. The Fe^{3+} content of the sodic amphibole is low to very low (with $Fe^{3+}/(Fe^{3+} + Al^{VI}) = 0.02$–$0.15$). Matrix grains ($X_{Mg} = 0.67$–$0.70$) are slightly more magnesian than inclusions ($X_{Mg} = 0.62$–0.65). Third, a few sodic-calcic amphiboles are developed at the garnet–glaucophane interfaces, ranging in composition from Si-poor barroisite to winchite.

Matrix epidote shows a restricted range of composition (from Ps45 to Ps50), and no core–rim zonation. Some epidote grains from the pseudomorphs have a lower Ps content (as low as Ps20) than matrix epidote. Chlorite grains are more magnesian in the pseudomorphs ($X_{Mg} = 0.62$–0.67) than at the garnet–glaucophane interfaces ($X_{Mg} = 0.56$–0.59). Paragonite is the only mica present, and is observed only in the pseudomorphs. Its chemistry is close

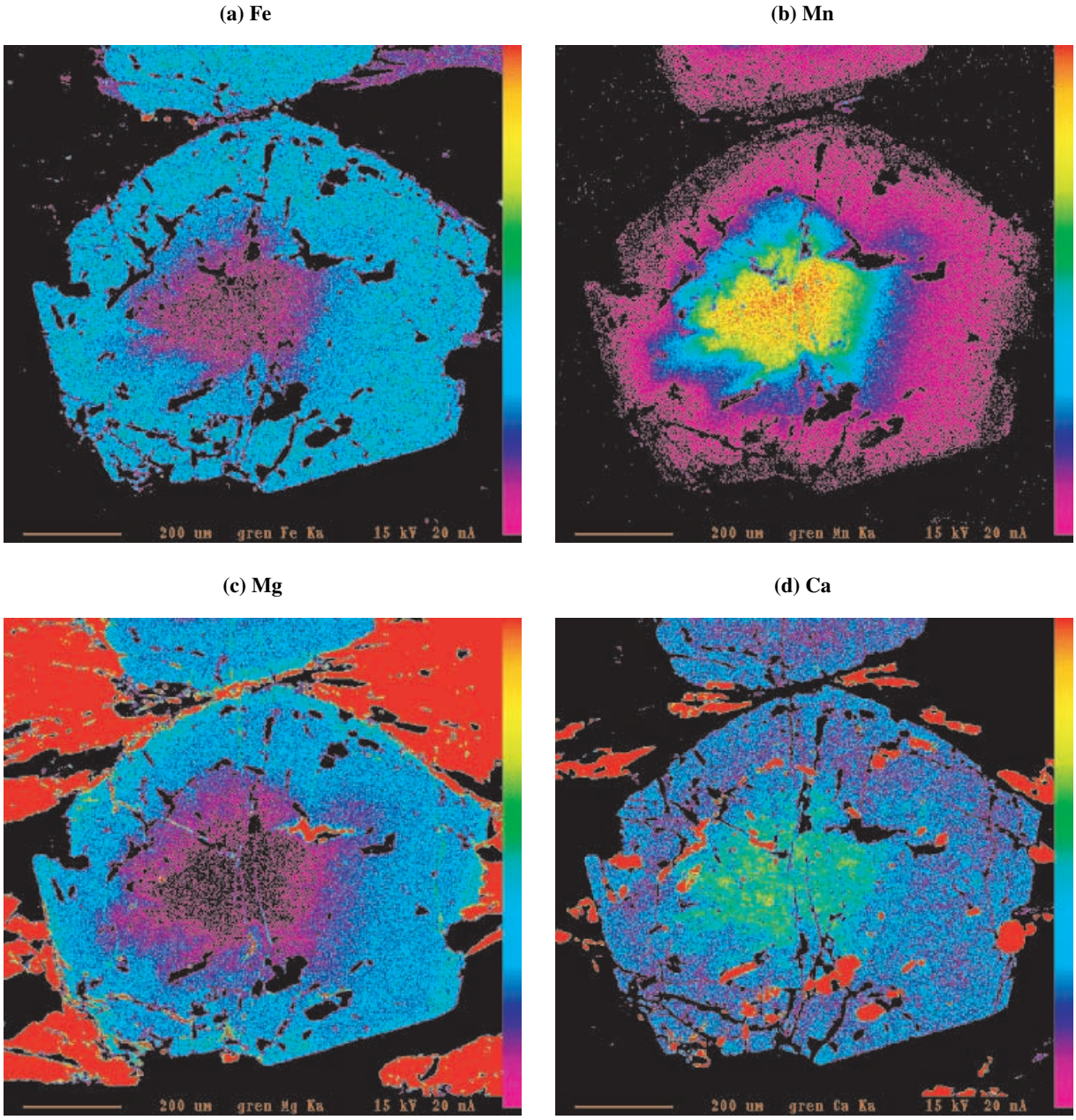

Fig. 5. X-ray element maps for Fe (a), Mn (b), Mg (c) and Ca (d) in a garnet from sample TRE 1. The garnet diameter is slighlty less than 1 mm. A few fractures cut across the garnet grain. Titanite inclusions and matrix grains are identified because of their very low Fe, Mn and Mg contents and a very high Ca content. Note how poorly foliated the titanite grains are in the garnet compared to the matrix. A large glaucophane inclusion, distinguished by its very high Mg content, is located in the outermost part of the Mn-rich core. The regular, smooth compositional gradient to the right, i.e. in an area devoid of inclusions, contrasts with the sharper gradient found in those area containing many inclusions.

to end-member, with a negligible margarite ($X_{Ca} < 0.01$) content and a low muscovite ($X_K = 0.05$–0.08) content. Plagioclase coexisting with chlorite at the garnet–glaucophane interfaces is a nearly pure albite, with maximum An and Or contents of 2 and 0.3 mole%, respectively. Titanite shows a low Al_2O_3 content, ranging from 0.9 to 2.3 wt%, with no core-to-rim zonation and a tendency toward lower Al_2O_3 contents of matrix grains with respect to inclusions within garnet. Rutile is nearly pure.

REACTION HISTORY OF LAWSONITE-BEARING BLUESCHISTS

Identification of the pseudomorphs

Because the glaucophane foliation is deflected around the pseudomorphs, and because they overgrow a

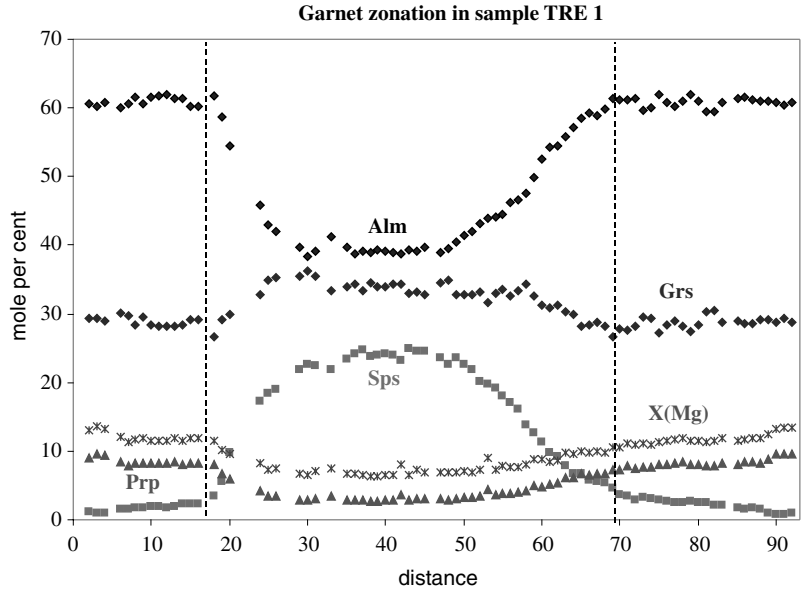

Fig. 6. Zoning profile through the same garnet grain as in Fig. 5. The traverse is made along an East-West line through the garnet core. Note the bell-shaped curve for spessartine, the increasing X_{Mg} from core to rim and the asymmetry of the compositional profile. Microprobe analyses of the core and the rim of this grain are shown in Table 1.

glaucophane-epidote foliation (Felix, 1972b), the pseudomorphed porphyroblasts must have been in equilibrium with glaucophane. The glaucophane oligoclase assemblage has never been reported previously and the stable coexistence of glaucophane and oligoclase is not predicted by petrogenetic grids calculated using thermodynamic databases (e.g. Evans, 1990). The experimentally determined stability field of oligoclase or, worse, andesine (Goldsmith, 1982) does not match the *P–T* conditions generally ascribed to the blueschist facies. It is therefore highly unlikely that Ca-bearing plagioclase rather than lawsonite was the original mineral, as proposed by Shelley & Bossière (1999). This hypothesis can therefore be rejected.

Although the interfacial angles of the pseudomorphs cannot be measured in the studied sample, the lozenge sections of the pseudomorphed mineral are well preserved. When measurable (Fig. 2), the interfacial angles are consistent with lawsonite (see Discussion in Felix & Fransolet, 1972). The breakdown products (chlorite, epidote and paragonite) are also consistent with the pseudomorphs being derived from lawsonite, as discussed below. A direct proof of the nature of the pseudomorphs in blueschists or eclogites would be to find partially transformed porphyroblasts, like those exceptional samples described in the Syros blueschists (Dixon, 1969, 1976; J. C. Schumacher, 2002, personal communication) or found in eclogite xenoliths from ultramafic pipes (Watson & Morton, 1969; Helmstaedt & Schulze, 1988).

The model systems NCFMASH and NCFMASHO

To identify the potential reactions involved in lawsonite growth and breakdown, *P–T* pseudosections were calculated, in the *P–T* window of interest, using the software THERMOCALC vs. 3.1 (Powell & Holland, 1985, 1988) and the internally consistent thermodynamic data set (Holland & Powell, 1998; modified May 14, 2001).

For the sake of clarity, only phases potentially in equilibrium with lawsonite were considered: garnet, glaucophane, chlorite, paragonite, clinozoisite/epidote, lawsonite, quartz and a H_2O fluid (see Appendix for the mixing models used). In the model system NCFMASH, generally appropriate for the study of metabasic rocks, these phases are in equilibrium along one stable univariant curve emanating from a stable NCFASH invariant point (cf. Will *et al.*, 1998). The bulk rock composition of the studied sample was calculated from the modal proportions and chemical compositions of the minerals considered in equilibrium (Table 2), and agrees well with the compositions of the Ile de Groix blueschists (see Felix, 1972b; Bernard-Griffiths *et al.*, 1986). However, the calculated NCFMASH *P–T* pseudosection (Fig. 7a) does not reproduce the inferred main syntectonic assemblage garnet–glaucophane–lawsonite–epidote. The reason for this may be (a) an erroneous identification of the equilibrium assemblage, (b) problematic thermodynamic data and/or mixing models used or, (c) inadequacy of the chosen model

Table 2. Modes and compositions of minerals used to determine the bulk composition used for calculation of pseudosections (see Appendix for the significance of the variables). Because THERMOCALC uses molar proportions, observed volume proportions of the peak mineral assemblage were converted using molar volume data from the THERMOCALC database. For calculations in the NCFMASH system pure clinozoisite instead of epidote solid solution was used.

Mineral	Composition	vol. %	mol. %
Grt	$x = 0.87$; $z = 0.31$	15	22
Gln	$x = 0.32$; $n = 0.97$	65	42
Ep	$x1 = 0.01$; $x3 = 0.5$	7	9
Lws	end-member	12	20
Qtz	end-member	1	7

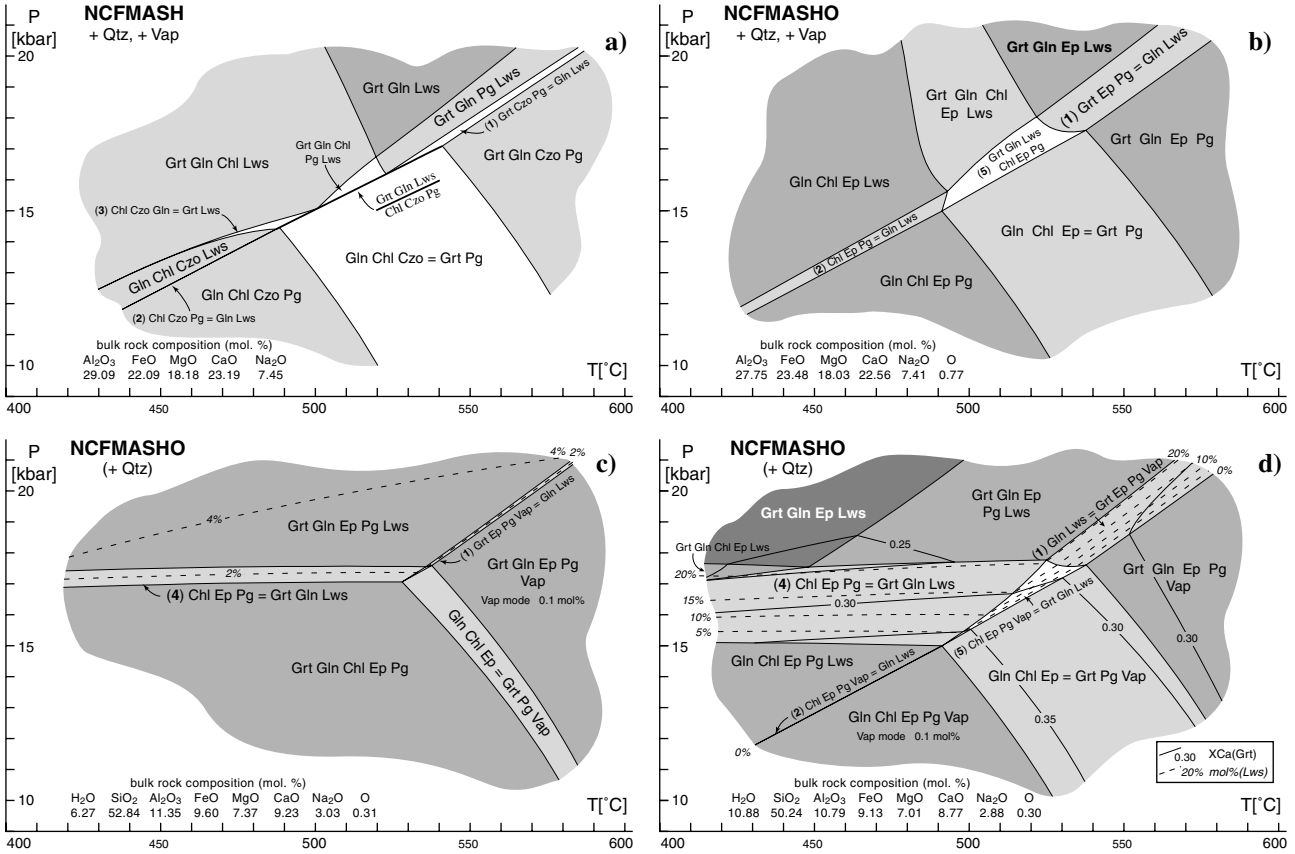

Fig. 7. *P–T* pseudosections calculated with THERMOCALC for the studied sample in the system (a) NCFMASH, (b–d) NCFMASHO. Quartz and H_2O fluid (Vap) are in excess in (a) and (b). In (c) and (d), neither water nor quartz are considered in excess, but quartz is present in all parageneses. The H_2O content was set so that about 0.1 mole % of free H_2O fluid is present in the stability field of Grt-Gln-Ep-Pg and Gln-Chl-Ep-Pg in (c) and (d), respectively. To facilitate the understanding of the continuous reactions, some relevant fields are labelled as reaction equilibria (e.g. Grt Czo Pg = Gln Lws). Light full lines in (d) are isopleths of X_{Ca} in garnet (= Ca/Ca + Fe + Mg). Light broken lines in (c) and (d) are isopleths of lawsonite mode.

system. Taking into account the important proportion (about 50%) of the pistacite end-member in epidote, the last solution seems the most appropriate, and a new pseudosection was calculated in the model system NCFMASHO (Fig. 7b). Manganese was not included in the model system, because it is strongly concentrated and isolated in garnet cores, making the bulk composition effective for the crystallization of the main syntectonic assemblage nearly Mn-free. On the other hand, it has to be borne in mind that the presence of Mn would stabilise garnet towards low-temperatures and pressures in the beginning of its growth. Fe^{3+} was considered to enter epidote only. Indeed, analysed glaucophane has very low Fe^{3+} contents (Table 1), interaction parameters of riebeckite with the other amphibole end-members are poorly constrained, other ferric minerals are absent and the lawsonite-bearing blueschists on Ile de Groix have generally a rather low Fe^{3+}/Fe^{2+} ratio (Felix, 1972a,b).

The lawsonite structure contains large amounts of H_2O and accordingly the reactions involving lawsonite have a strong hydration/dehydration character. Consequently, and due to the limited amount of free water available in the pores of deep-seated rocks (e.g. Fyfe *et al.*, 1978; Jamtveit & Yardley, 1997), it may be inappropriate to consider a system with water in excess. Therefore, pseudosections have also been calculated for bulk compositions with a given amount of H_2O (Fig. 7c,d). This is not easy to model satisfactorily, since free fluid tends to escape from rocks, modifying continuously the bulk composition in terms of H_2O. In the examples below, the H_2O contents were fixed arbitrarily so that the parageneses of interest are just H_2O-saturated, i.e. contain a minimum amount (about 0.1 mole %) of free H_2O fluid.

Growth of the lawsonite porphyroblasts

Three main constraints are to be satisfied, namely (i) that lawsonite grew in an epidote-bearing rock (ii) that lawsonite grew later than garnet (Fig. 3), and (iii) that the main syndeformational assemblage was Grt–Gln–Ep–Lws, without paragonite (quartz being present in all assemblages).

The first possibility for entering the Grt–Ep–Lws–Gln stability field (Fig. 7b) would be a decrease in

temperature during the decompression, as suggested by Barnicoat & Fry (1986) in the Alpine blueschists. Lawsonite would have appeared due to the continuous reaction

$$\text{Grt} + \text{Ep} + \text{Pg} + \text{Vap} = \text{Gln} + \text{Lws} \quad (1)$$

However, assuming that only very little water fluid could be present in the initial assemblage Grt–Gln–Ep–Pg (Fig. 7c), cooling to unreasonably low temperatures (*c.* 130 °C) would be necessary to reach the Grt–Gln–Ep–Lws stability field. Moreover, only slightly more than 4 molar % of lawsonite is formed during this evolution, much less than the proportion observed in the rock (about 20 mole %, cf. Table 2). To form the observed quantity of lawsonite, and at reasonable *P–T* conditions, this reaction would necessitate an infiltration of H_2O into the rock. Finally, this reaction involves garnet resorption during lawsonite growth, for which no evidence has been found. We consider therefore that this reaction is not a plausible solution.

A second possibility is that lawsonite growth was possible during the prograde history, with increasing pressure, due to the reaction (Fig. 7; cf. fig. 1 in Will *et al.*, 1998)

$$\text{Chl} + \text{Ep} + \text{Pg} + \text{Vap} = \text{Gln} + \text{Lws}, \quad (2)$$

or

$$\text{Chl} + \text{Ep} + \text{Gln} + \text{Vap} = \text{Grt} + \text{Lws}. \quad (3)$$

Both equilibria are very close to one another in the NCFASH and NCFMASH systems and coalesce to form a divariant field in NCFMASHO (Fig. 7). A number of reasons suggest that this possibility is reasonable. First, assuming again that the initial assemblage Gln–Chl–Ep–Pg (Fig. 7d) is just saturated with H_2O fluid, with increasing pressure the rock would develop the inferred Grt–Gln–Ep–Lws assemblage with more than 20 molar % of lawsonite. Due to the small initial amount of free water, only about 0.2 molar % of lawsonite grows upon crossing the continuous hydration reaction (2), whereas 20 mole % is formed by the fluid-absent continuous reaction

$$\text{Chl} + \text{Ep} + \text{Pg} = \text{Grt} + \text{Gln} + \text{Lws}, \quad (4)$$

due mostly to the consumption of chlorite, the H_2O component being transferred from chlorite to lawsonite with increasing pressure. Second, this reaction is consistent with the textural observations, namely lawsonite growth in an epidote-bearing rock and contemporaneous growth of lawsonite and garnet. The early beginning of garnet growth compared to lawsonite, not predicted by the pseudosection, can be accounted for easily by the stabilisation of garnet towards lower *P–T* conditions due to the concentration of Mn. Finally, it is comforting to note that the predicted compositions of garnet in equilibrium with lawsonite, glaucophane and epidote (Fig. 7d) are close to those measured in the rock. Moreover, the observed decrease in grossular content from core to rim (Figs 5 & 6) is also consistent with an increase in pressure at the time of lawsonite growth.

Breakdown of the lawsonite porphyroblasts

Breakdown of the porphyroblasts may occur through decompression or heating. The large amount of chlorite present in the pseudomorphs suggests that decompression played a major role. In addition to reactions (2) and (4), the divariant equilibrium

$$\text{Grt} + \text{Gln} + \text{Lws} = \text{Chl} + \text{Ep} + \text{Pg} + \text{Vap} \quad (5)$$

is a potential candidate for lawsonite breakdown. All three reactions produce chlorite, epidote and paragonite, which is consistent with the observed mineralogy of the lawsonite pseudomorphs. The main difference between these reactions is that no vapour is produced through reaction (4), whereas it is liberated by reactions (2) and (5). Which reaction plays a major role is a subtle effect of the H_2O content of the rock. In rocks with low H_2O content most lawsonite is consumed through the fluid-absent reaction (4), whereas reactions (2) and (5) play a more important role in rocks rich in H_2O.

According to Shelley & Bossière (1999), the breakdown products represent retrogression into the greenschist facies. The above model shows that Chl–Ep–Pg are stable with glaucophane, thus indicating that the breakdown products are consistent with the blueschist facies. Moreover, lawsonite breakdown need not liberate a copious amount of water, as suggested by Shelley & Bossière (1999). It is thus not a problem to explain the lack of a more general retrogression of the glaucophane–epidote matrix.

DISCUSSION

Sensitivity of the pseudosections

To test the stability of the model, we have calculated pseudosections over a range of bulk compositions obtained by modifying the estimated proportions of garnet, glaucophane and lawsonite in a range 5–25, 55–75 and 5–25 vol%, respectively (cf. Table 2). This results in displacements of the central divariant field by up to 1.3 kbar and about 20 °C, but alters neither the relative position nor the shape/slope of the trivariant equilibria. In runs with higher garnet and lower glaucophane or lower lawsonite content (composition (a) in Fig. 8), paragonite is consumed before vapour or chlorite over the trivariant fields (1) and (4). This leads to the appearance of a new trivariant equilibrium Grt-Gln–Lws–Chl–Ep–Vap and to the stabilisation of the Grt–Gln–Ep–Lws assemblage in H_2O-saturated conditions. The vapour-absent Grt-Gln-Ep-Lws field is shifted to higher pressures (Fig. 8). On the other hand, this latter field was displaced to much lower temperatures, along the Chl-out limit of the Grt–Gln–Lws–Chl–Ep–Pg equilibrium (4) in runs with increased

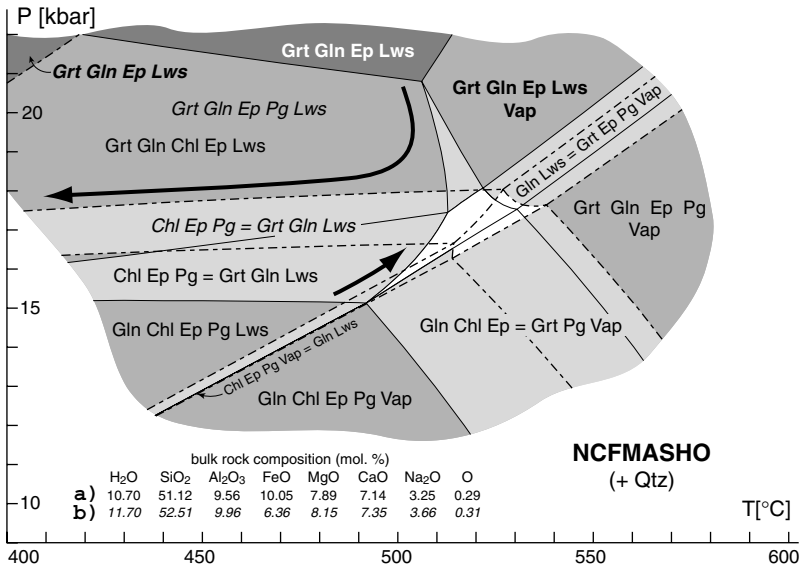

Fig. 8. Two superposed *P–T* pseudosections calculated to demonstrate the influence of changing bulk composition. Field limits are full lines for composition (a) obtained considering a lower proportion of lawsonite (Grt:Gln:Ep:Lws:Qtz = 16:71:7:5:1 vol%) compared to the composition used in Fig. 7(d) (cf. Table 2). A similar diagram results from increasing the amount of garnet at the expense of glaucophane. Broken lines (and fields labelled in italic) show the result for a composition with increased glaucophane and less garnet (b; Grt:Gln:Ep:Lws:Qtz = 5:75:7:12:1 vol%). Thick black arrows indicate the trends of major field displacements. See text for further discussion.

amounts of glaucophane or lawsonite (composition (b) in Fig. 8). Despite these temperature variations, the minimum pressure where the Grt–Gln–Ep–Lws (with or without vapour) assemblage becomes stable remains invariably between 17 and 18 kbar. Therefore, even relatively important bulk composition modifications do not change the general appearance of the pseudosection. The trivariant fluid-absent equilibrium (4) remains the main producer of lawsonite, whereas the amount of lawsonite formed by reaction (2) depends essentially on the initial proportion of free H_2O fluid.

Except for glaucophane, the choice of mixing models has relatively little effect on the exact *P–T* position of the equilibria. Even replacing regular mixing models by ideal ones for garnet, epidote or chlorite results in a maximum displacement of the equilibria of some 15 °C and 0.5 kbar only. The nonideality of glaucophane is modelled using the Darken's Quadratic Formalism (Powell, 1987; Will & Powell, 1992; see Appendix). Changing the *I* parameters for fictive end-members of ± 10 kJ (nearly three times the 2σ uncertainties of Will & Powell, 1992) displaces equilibria of at most ± 0.7 kbar, but up to ± 80 °C. However, these large temperature variations affect the paragonite-out boundaries only, especially the five-variant Grt–Gln–Ep–Lws field, due to the changes in the glaucophane composition. Positions of other equilibria are modified by less than ± 20 °C.

Clearly, the exact position of the various fields in pseudosections depends to a more or less important extent on (a) the bulk composition (b) the mixing models for solid solutions and (c) the thermodynamic database used. On the other hand, the relative position of the fields and the slope of the reactional equilibria are robust and reliable. Consequently, we regard such model diagrams as a framework for interpretation of textures and estimation of relative *P–T* differences between samples or units, rather than as a tool for precise determination of equilibrium *P–T* conditions.

Lawsonite growth in epidote-bearing blueschists

Experimental data as well as numerical models (e.g. Evans, 1990; Kerrick & Connolly, 2001; and the above calculations) show that the coexistence of glaucophane and lawsonite indicates lower temperatures than the assemblage glaucophane–epidote. This does not mean that the two assemblages strictly define two separate *P–T* fields, because epidote can be stable with lawsonite in a large range of *P–T* conditions. The late development of lawsonite in an epidote-bearing blueschist is reported in some localities (e.g. Felix & Fransolet, 1972; Barnicoat & Fry, 1986) and was interpreted as recording decreasing temperatures at the beginning of the exhumation history (Barnicoat & Fry, 1986). Another explanation, advocated in this paper on the basis of our observations in the Ile de Groix blueschists, is a growth of lawsonite during the prograde, up-pressure and up-temperature, history. The basic consequence of this model is a transfer of the H_2O component from the fluid phase and then from chlorite into lawsonite, which coexists with epidote at high pressure in a fluid-absent rock. The H_2O component can thus be carried down a subduction zone up to ultra-high pressures (e.g. Poli & Schmidt, 2002), where lawsonite breaks down (to omphacite–clinozoisite–kyanite–coesite), or can be released during decompression, also recorded by lawsonite breakdown (to epidote–chlorite–paragonite–quartz).

P–T history of the Ile de Groix blueschists

According to our calculations (Fig. 7d), peak *P–T* conditions in the Upper Unit of the Ile de Groix were at about 18–20 kbar, 450 °C, a conclusion in agreement with a previous estimate (Bosse *et al.*, 2002). This latter work can be considered as truly independent of the present work (although having in common one

author) because it is based on a different set of parageneses in a different set of rocks (garnet–chloritoid–glaucophane in metapelites) and because the *P–T* conditions are estimated using a different set of thermodynamic parameters and solid solution models (TWQ in Bosse *et al.*, 2002 vs. THERMOCALC in this paper). This gives some confidence in the absolute values here reported. However, several *P–T* histories have been proposed for the Ile de Groix blueschists. Three types of discrepancies have been encountered, that need to be carefully evaluated with respect to the meaning of the pseudomorphs.

First, according to some estimates, the *P–T* conditions at peak pressure were at higher temperatures than the lawsonite stability field (Audren & Triboulet, 1984; Djro *et al.*, 1989; Audren *et al.*, 1993). The pseudomorphs are thus interpreted as lawsonite porphyroblasts that broke down before peak *P–T* conditions (Audren & Triboulet, 1984; Djro *et al.*, 1989). However, our textural and numerical analyses indicate that lawsonite growth occurred during the prograde *P–T* path, close to peak *P–T* conditions, and that lawsonite was stable at peak *P–T* conditions.

Second, other discrepancies are related to the shape of the *P–T* path. The *P–T* history of the sample is characterized by a clockwise *P–T* path, that culminated at about 18–20 kbar, 450 °C (Fig. 9). In our interpretation, lawsonite growth results from a hydration reaction followed by a fluid-absent reaction that took place at the end of the up-pressure path. Ductile deformation took place during lawsonite growth. Decompression occurred after the cessation of ductile deformation, and resulted in the breakdown of lawsonite, then garnet. As stressed by Barrientos & Selverstone (1993), lawsonite breakdown is a dehydration reaction, hence its completeness, but garnet breakdown necessitates introduction of H_2O into the rock, hence its limited extent. In contrast to our interpretation, Audren *et al.* (1993) suggested that the pseudomorphs could represent former lawsonite porphyroblasts that have grown after the blueschist facies event, when the stable amphibole was a green, calcic, amphibole. This hypothesis is contradicted by the textural observations (Fig. 3). Indeed, the glaucophane foliation is deflected around the porphyroblats, implying their pre- or syn-kinematic growth with respect to glaucophane. Shelley & Bossière (1999; path 2 of their fig. 1b) advocated a late growth of lawsonite (if indeed the pseudomorphs are assumed to be after lawsonite) during a cooling stage at high pressure. This possibility, which is similar to the one proposed by Barnicoat & Fry (1986) in the Alps, has been already discussed and rejected in the case of the Ile de Groix blueschists (see above).

Third, while most people recognize only one tectonothermal cycle in the Ile de Groix blueschists (Barrientos, 1992; Shelley & Bossière, 1999; Bosse *et al.*, 2002), some have identified two superposed cycles (Schulz *et al.*, 2001). The first cycle culminated in the blueschist facies and the second cycle culminated at lower pressures and higher temperatures than the first cycle. Specifically, the second cycle would have culminated in the locality where sample TRE 1 has been sampled at 8–10 kbar and 700–800 °C. Because the growth zoning of the garnet does not show resorption followed by a new phase of growth, and because the growth zoning associated with the first cycle only is recorded (remember the presence of epidote, actinolite and glaucophane inclusions), the hypothesis of Schulz *et al.* (2001) is considered unlikely.

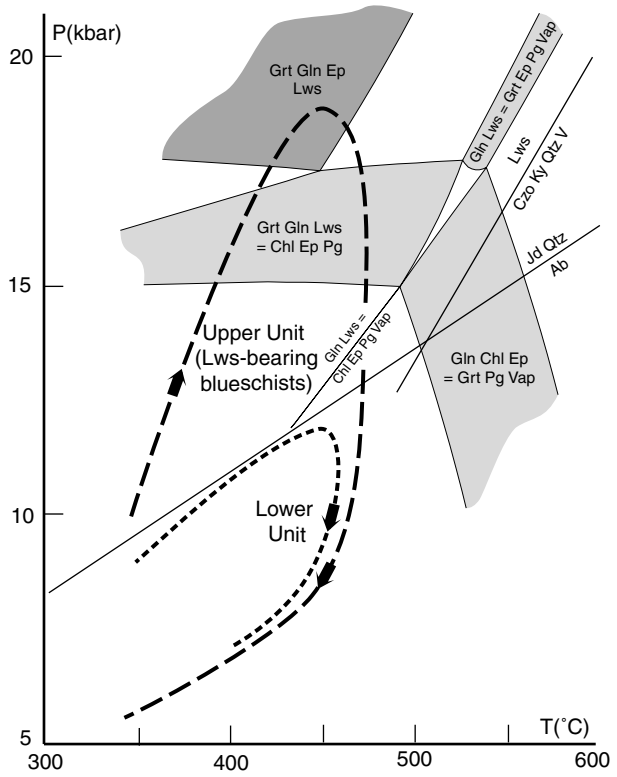

Fig. 9. *P–T* history of the Ile de Groix blueschists, based on the lawsonite-bearing samples. Key equilibrium curves are reported after Holland (1980), Newton & Kennedy (1963) and the calculated pseudosection (Fig. 7d).

Differences between units

The distribution of the lawsonite pseudomorphs at the scale of the island is to some extent counterintuitive. Indeed, lawsonite pseudomorphs are commonly found in the Upper Unit (Fig. 1), i.e. in the higher-grade unit. On the contrary, pseudomorphs are very rare in the Lower Unit (Fig. 1), and occur in rocks that are essentially consisting of a Fe-glaucophane, ankerite and epidote, hence present a different bulk-rock chemistry from those investigated in this study. Mafic rocks with similar bulk compositions are present in both units, but they are devoid of lawsonite pseudomorphs in the Lower Unit. Thus, the distribution of the lawsonite pseudomorphs at the scale of the island is not

controlled by a difference in bulk-rock chemistry of the protoliths, but by a difference in *P–T* conditions during the blueschist facies event (or a difference in *P–T* path).

The reactions controlling lawsonite growth offer a likely explanation for its distribution (Fig. 9). Because lawsonite can develop in epidote-bearing blueschists at increasing pressure, it can be assumed that peak pressures in the Lower Unit did not exceed those permitting lawsonite growth in mafic rocks of basaltic composition. Peak pressures were thus lower in the Lower Unit than in the Upper Unit, supporting the existence of a thrust contact between the two units (Bosse *et al.*, 2002).

CONCLUSIONS

The main conclusions of this study are:

(**1**) Rhomb-shaped pseudomorphs essentially consisting of chlorite, epidote and paragonite from the Ile de Groix blueschists represent former lawsonite porphyroblasts, a result consistent with previous studies (Cogné *et al.*, 1966; Felix, 1972a, 1972b; Felix & Fransolet, 1972). Other possibilities for the pseudomorphed phase, like plagioclase (Shelley & Bossière, 1999), are dismissed.

(**2**) Lawsonite porphyroblasts overgrew a foliated matrix consisting of garnet, glaucophane and epidote. Lawsonite growth results from a hydration and/or fluid-absent reaction occurring at increasing *P–T*, culminating at about 18–20 kbar, 450 °C, i.e. by a reaction transferring much of the H_2O component from chlorite to lawsonite (Fig. 7). This would allow water to be carried down the subduction zone up to about 100 kbar, i.e. about 300 km (Poli & Schmidt, 2002). This was not the case of the Ile de Groix blueschists, where lawsonite breakdown occurred in the early stages of exhumation.

(**3**) Lawsonite pseudomorphs in the Ile de Groix blueschists are not randomly distributed throughout the island (Fig. 1). They occur in the eastern half of the island, in the higher-grade Upper Unit (Bosse *et al.*, 2002). *P–T* conditions in the western part of the island were also located in the stability field of lawsonite, but lawsonite development is much less extensive because pressures were lower than in the Upper Unit (Fig. 9). Paradoxically, this explains why lawsonite is more common in the higher-grade blueschists compared to the lower-grade blueschists from the Ile de Groix. It also indicates that some growth reactions, especially reaction (4), for lawsonite in epidote blueschists are potential geobarometers.

ACKNOWLEDGEMENTS

Thanks are due to V. Bosse for her help during the course of this study. Financial support for this study was provided by Géofrance3D-Armor2. Many thanks are due to J. Brady, G. Ernst and S. Poli for their reviews.

REFERENCES

Audren, C. & Triboulet, C., 1984. Métamorphisme et déformation dans la ceinture de haute pression de l'Ile de Groix (Bretagne méridionale). *Bulletin de la Société Géologique et Minéralogique de Bretagne, (C)*, **16,** 61–70.

Audren, C., Triboulet, C., Chauris, L,, *et al.*, 1993. *Notice Explicative de la Feuille Ile de Groix Á 1/*25000 (Carte Géologique). BRGM, Orléans.

Barnicoat, A. C. & Fry, N., 1986. High-pressure metamorphism of the Zermatt-Saas ophiolite zone, Switzerland. *Journal of the Geological Society of London*, **143,** 607–618.

Barrientos, X., 1992. Petrology of coexisting blueschists and greenschists, Ile de Groix, France: implications for preservation of blueschists. *PhD Thesis*, *Harvard University, Cambridge, MA, USA*.

Barrientos, X. & Selverstone, J., 1993. Infiltration vs. thermal overprinting of epidote blueschists, Ile de Groix, France. *Geology*, **21,** 69–72.

Barrois, C., 1883. Mémoire sur les schistes métamorphiques de l'île de Groix. *Annales de la Société Géologique Du Nord*, **XI,** 18–71.

Bearth, P., 1973. Gesteins- und Mineralparagenesen aus den Ophiolithen von Zermatt. *Schweizerische Mineralogische und Petrographische Mitteilungen*, **53,** 299–334.

Bernard-Griffiths, J., Carpenter, M. S. N., Peucat, J.-J. & Jahn, B.-M., 1986. Geochemical and isotopic characteristics of blueschist facies rocks from the Ile de Groix, Armorican Massif (northwest France). *Lithos*, **19,** 235–253.

Bosse, V., Ballèvre, M. & Vidal, O., 2002. Ductile thrusting recorded by the garnet isograd from blueschist-facies metapelites of the Ile de Groix, Armorican Massif, France. *Journal of Petrology*, **43,** 485–510.

Cannic, S., Lardeaux, J.-M., Mugnier, J.-L. & Hernandez, J., 1996. Tectono-metamorphic evolution evolution of the Roignais-Versoyen Unit (Valaisan domain, France). *Eclogae Geologicae Helvetiae*, **89,** 321–343.

Caron, J.-M., 1977. Lithostratigraphie et tectonique des Schistes lustrés dans les Alpes cottiennes septentrionales et en Corse orientale. *Sciences Géologiques*, **48,** 1–326.

Carpenter, M. S. N., 1976. Petrogenetic study of the glaucophane schists and associated rocks from the Ile de Groix, Brittany, France. *PhD Thesis*, University of Oxford, Oxford.

Carson, C. J., Powell, R. & Clarke, G. L., 1999. Calculated mineral equilibria for eclogites in CaO-Na_2O-FeO-MgO-Al_2O_3-SiO_2–H_2O: application to the Pouébo Terrane, Pam Peninsula, New Caledonia. *Journal of Metamorphic Geology*, **17,** 9–24.

Chatterjee, N. D., Johannes, W. & Leistner, H., 1984. The system CaO-Al_2O_3-SiO_2-H_2O: new phase equilibria data, some calculated phase relations, and their petrological applications. *Contributions to Mineralogy and Petrology*, **88,** 1–13.

Cogné, J., Jeannette, D. & Ruhland, M., 1966. L'Ile de Groix: étude structurale d'une série métamorphique à glaucophane en Bretagne méridionale. *Bulletin du Service de la Carte Géologique d'Alsace-Lorraine*, **19,** 41–95.

Compagnoni, R., 1977. The Sesia-Lanzo zone: high-pressure – low-temperature metamorphim in the Austroalpine continental margin. *Rendiconti della Società Italiana di Mineralogia e Petrologia*, **33,** 335–374.

Deer, W. A., Howie, R. A. & Zussman, J., 1986. *Rock-Forming Minerals*, **Vol. 1B**: Disilicates and Ring Silicates, 2nd edn. Longman Scientific and Technical, Harlow.

Dixon, J. E., 1969. The metamorphic rocks of Syros, Greece. PhD, Cambridge University (unpub.).

Dixon, J. E., 1976. Glaucophane schists of Syros, Greece *Bulletin de la Société Géologique de France*, **7,** XVIII, 280 (Abstract).

Djro, C., Triboulet, C. & Audren, C., 1989. Les chemins pression-température-temps-déformation-espace (P-T-t-d-e) dans les micaschists associés aux schistes bleus de l'Ile de Groix, Bretagne méridionale, France. *Schweizerische Mineralogische und Petrographische Mitteilungen*, **69,** 73–90.

Dobretsov, N. L., Sobolev, V. S., Sobolev, N. V. & Khlestov, V. V., 1974. *The Facies of Regional Metamorphism at High*

Pressure (English Translation by Brown, D.A., 1975. ANU Press, Canberra).

Domanik, K. J. & Holloway, J. R., 1996. The stability and composition of phengitic muscovite and associated phases from 5.5 to 11 Gpa: Implications for deeply subducted sediments. *Geochimica et Cosmochimica Acta*, **60,** 4133–4150.

Ellenberger, F., 1960. Sur une paragenèse éphémère à lawsonite et glaucophane dans le métamorphisme alpin de Haute-Maurienne (Savoie). *Bulletin de la Société Géologique de France*, **7,** 190–194.

Evans, B. W., 1990. Phase relations of epidote-blueschists. *Lithos*, **25,** 3–23.

Felix, C., 1972a. Interprétation d'une paragenèse à glaucophane-épidote/lawsonite-grenat dans les glaucophanoschistes plurifaciels de l'Ile de Groix (Morbihan, France). *Comptes-Rendus de l'Académie des Sciences de Paris, (D)*, **275,** 317–320.

Felix, C., 1972b. Etude structuro-minéralogique des pseudomorphes de présumée lawsonite des glaucophanoschistes de l'île de Groix (Bretagne – France): considérations sur la possibilité d'une paragenèse à glaucophane et lawsonite. *Annales de la Société Géologique de Belgique*, **95,** 345–391.

Felix, C. & Fransolet, A. M., 1972. Pseudomorphes à épidote s.l., paragonite, muscovite s.l., chlorite, albite, … de porphyroblastes de lawsonite (?) dans les glaucophanites de l'île de Groix (Bretagne – France). *Annales de la Société Géologique de Belgique*, **95,** 323–334.

Forbes, R. B., Evans, B. W. & Thurston, S. P., 1984. Regional progessive high-pressure metamorphism, Seward Peninsula, Alaska. *Journal of Metamorphic Geology*, **2,** 43–54.

Fry, N., 1973. Lawsonite pseudomorphs in Tauern greenschist. *Mineralogical Magazine*, **39,** 121–122.

Fry, N. & Barnicoat, A. C., 1987. The tectonic implications of high-pressure metamorphism in the western Alps. *Journal of Metamorphic Geology*, **144,** 653–659.

Fry, N. & Fyfe, W. S., 1971. On the significance of the eclogite facies in Alpine metamorphism. *Verhandlungen der Geologischen Bundesanstalt*, **2,** 257–265.

Fyfe, W. S., Price, N. J. & Thompson, A. B., 1978. *Fluids in the Earth's Crust Developments in Geochemistry, 1.* Elsevier, Amsterdam.

Goldsmith, J. R., 1982. Plagioclase stability at elevated temperatures and water pressures. *American Mineralogist*, **67,** 653–675.

Green, D. H., Lockwood, J. P. & Kiss, E., 1968. Eclogite and almandine-jadeite-quartz rock from the Guajira Peninsula, Colombia, South America. *American Mineralogist*, **53,** 1320–1335.

Grevel, K.-D., Schoenitz, M., Skrok, V., Navrotsky, A. & Schreyer, W., 2001. Thermodynamic data of lawsonite and zoisite in the system CaO-Al_2O_3-SiO_2-H_2O based on experimental phase equilibria and calorimetric work. *Contributions to Mineralogy and Petrology*, **142,** 298–308.

Heinrich, W. & Althaus, E., 1988. Experimental determination of the reaction 4lawsonite + 1albite = 1paragonite + 2zoisite + quartz + $6H_2O$ and 4lawsonite + 1albite = 1paragonite + 2zoisite + quartz + $6H_2O$. *Neues Jahrbuch für Mineralogie Monatshefte*, **11,** 516–528.

Helmstaedt, H. & Schulze, D. J., 1988. Eclogite-facies ultramafic xenoliths from Colorado Plateau diatreme breccias: comparison with eclogites in crustal environments, evaluation of the subduction hypothesis, and implications for eclogite xenoliths from diamondiferous kimberlites. In: *Eclogites and Eclogite-Facies Rocks, Developments in Petrology, 12* (Smith, D. C., ed.), pp. 387–450. Elsevier, Amsterdam.

Höck, V. V., 1974. Lawsonitpseudomorphosen in den Knotenschiefern der Glocknergruppe. *Karinthin*, **71,** 110–119.

Holland, T. J. B., 1980. The reaction albite = jadeite + quartz determined experimentally in the range 600 °C to 1200 °C. *American Mineralogist*, **65,** 129–134.

Holland, T. J. B. & Powell, R., 1998. An internally consistent thermodynamic data set for phases of petrological interest. *Journal of Metamorphic Geology*, **16,** 309–343.

Jamtveit, B. & Yardley, B. W. D., 1997. *Fluid Flow and Transport in Rocks Mechanisms and Effects*. Chapman & Hall, London.

Kerrick, D. M. & Connolly, J. A. D., 2001. Metamorphic devolatilization of subducted oceanic metabasalts: implications for seismicity, arc magmatism and volatile recycling. *Earth and Planetary Science Letters*, **189,** 19–29.

Leake, B. E. *et al*., 1997. Nomenclature of amphiboles. Report of the Subcommitte on amphiboles of the International Mineralogical Association commission on new minerals and mineral names. *European Journal of Mineralogy*, **9,** 623–651.

Liu, J., Bohlen, S. R. & Ernst, W. G., 1996. Stability of hydrous phases in subducting oceanic crust. *Earth and Planetary Science Letters*, **143,** 161–171.

Makanjuola, A. A. & Howie, R. A., 1972. The mineralogy of the glaucophane schists and associated rocks from île de Groix, Brittany, France. *Contributions to Mineralogy and Petrology*, **35,** 85–118.

Martin, S. & Tartarotti, P., 1989. Polyphase HP metamorphism in the ophiolitic glaucophanites of the lower St. Marcel valley (Aosta, Italy). *Ofioliti*, **14,** 135–156.

Mével, C. & Kiénast, J.-R., 1980. Chromian jadeite, phengite, pumpellyite and lawsonite in a high-pressure metamorphosed gabbro from the French Alps. *Mineralogical Magazine*, **43,** 979–984.

Miyajima, H., Matsubara, S., Miyawaki, R. & Ito, K., 1999. Itoigawaite, a new mineral, the Sr analogue of lawsonite, in jadeitite from the Itoigawa-Ohmi district, central Japan. *Mineralogical Magazine*, **63,** 909–916.

Newton, R. C. & Kennedy, G. C., 1963. Some equilibrium reactions in the join $CaAl_2Si_2O_6 - H_2O$. *Journal of Geophysical Research*, **68,** 2967–2983.

Nitsch, K.-H., 1972. Das P-T-XCO_2 – Stabilitätsfeld von Lawsonit. *Contributions to Mineralogy and Petrology*, **34,** 116–134.

Okamoto, K. & Maruyama, S., 1999. The high-pressure synthesis of lawsonite in the MORB + H_2O system. *American Mineralogist*, **84,** 362–373.

Okrusch, M., Seidel, E. & Davis, E. N., 1978. The assemblage jadeite-quartz in the glaucophane rocks of Sifnos (Cyclades Archipelago, Greece). *Neues Jarhbuch für Mineralogie Abhandlungen*, **132,** 284–308.

Ono, S., 1998. Stability limits of hydrous minerals in sediment and mid-ocean ridge basalt compositions: Implications for water transport in subduction zones. *Journal of Geophysical Research*, **103,** 18 253–18 267.

Patrick, B. E. & Evans, B. W., 1989. Metamorphic evolution of the Seward Peninsula Blueschist terrane. *Journal of Petrology*, **30,** 531–555.

Pawley, A. R., 1994. The pressure and temperature stability limits of lawsonite: implications for H_2O recycling in subduction zones. *Contributions to Mineralogy and Petrology*, **118,** 99–108.

Pierrot, R., Chauris, L., Laforêt, C. & Pillard, F., 1980. *Inventaire Minéralogique de la France No 9: Morbihan (56)* BRGM, Orléans.

Pognante, U., 1989. Tectonic implications of lawsonite formation in the Sesia zone (Western Alps). *Tectonophysics*, **162,** 219–227.

Poli, S. & Schmidt, M. W., 1998. The high-pressure stability of zoisite and phase relationships of zoisite-bearing assemblages. *Contributions to Mineralogy and Petrology*, **130,** 162–175.

Poli, S. & Schmidt, M. W., 2002. Petrology of subducted slabs. *Annual Review of Earth and Planetary Sciences*, **30,** 207–235.

Powell, R., 1987. Darken's quadratic formalism and the thermodynamics of minerals. *American Mineralogist*, **72,** 1–11.

Powell, R. & Holland, T. J. B., 1985. An internally consistent dataset with uncertainties and correlations: 1. Methods and a worked example. *Journal of Metamorphic Geology*, **3,** 327–342.

Powell, R. & Holland, T. J. B., 1988. An internally consistent dataset with uncertainties and correlations: 3. Applications to geobarometry, worked examples and a computer program. *Journal of Metamorphic Geology*, **6,** 173–204.

Powell, R. & Holland, T. J. B., 2002. Course Notes for 'THERMOCALC Workshop 2002: Calculating Metamorphic Phase Equilibria' (Barcelona), on CD-ROM.
Quinquis, H. & Choukroune, P., 1981. Les schistes bleus de l'île de Groix dans la chaîne hercynienne: implications cinématiques. *Bulletin de la Société Géologique de France*, **7,** 409–418.
Reynard, B. & Ballèvre, M., 1987. Coexisting amphiboles in an eclogite from the Western Alps: new constraints on the miscibility gap between sodic and calcic amphiboles. *Journal of Metamorphic Geology*, **6,** 333–350.
Schmidt, M. W., 1995. Lawsonite: upper pressure stability and formation of higher density hydrous phases. *American Mineralogist*, **80,** 1286–1292.
Schmidt, M. W. & Poli, S., 1994. The stability of lawsonite and zoisite at high pressures: experiments in CASH to 92 kbar and implications for the presence of hydrous phases in subducted lithosphere. *Earth and Planetary Science Letters*, **124,** 105–118.
Schulte, B. & Sindern, S., 2002. K-rich fluid metasomatism at high-pressure metamorphic conditions: Lawsonite decomposition in rodingitized ultrmafite of the Maksyutovo Complex, Southern Urals (Russia). *Journal of Metamorphic Geology*, **20,** 529–541.
Schulz, B., Triboulet, C., Audren, C., Pfeifer, H.-R. & Gilg, A., 2001. Two-stage prograde and retrograde Variscan metamorphism of glaucophane eclogites, blueschists and greenschists from the ile de Groix (Brittany, France). *International Journal of Earth Sciences*, **90,** 871–889.
Shelley, D. & Bossière, G., 1999. Ile de Groix: retrogression and structural developments in an extensional régime. *Journal of Structural Geology*, **21,** 1441–1445.
Sherlock, S. C. & Okay, A. I., 1999. Oscillatory zoned chrome lawsonite in the Tavsanli Zone, northwest Turkey. *Mineralogical Magazine*, **63,** 687–692.
Sicard, E., Potdevin, J.-L. & Caron, J.-M., 1984. Coexistence de lawsonite et de pseudomorphoses à pyrophyllite et kaolinite dans les Schistes lustrés corses: rôle des fluides. *Comptes-Rendus de l'Académie des Sciences de Paris*, **II** (298)**,** 453–458.
Smelik, E. A. & Veblen, D. R., 1992. Exsolution of Ca-amphibole from glaucophane and the miscibility gap between sodic and calcic amphiboles. *Contributions to Mineralogy and Petrology*, **112,** 178–195.
Thurston, S. P., 1985. Structure, petrology and metamorphic history of the Nome Group blueschist terrane, Salmon Lake area, Seward Peninsula, Alaska. *Geological Society of America Bulletin*, **96,** 600–617.
Triboulet, C., 1974. Les glaucophanites et roches associées de l'île de Groix (Morbihan, France): étude minéralogique et pétrogénétique. *Contributions to Mineralogy and Petrology*, **45,** 65–90.
Van der Plas, L., 1959. Petrology of the northern Adula region, Switzerland (with particular reference to glaucophane-bearing rocks). *Leidse Geologische Mededelingen*, **24,** 415–602.
Watson, K. D. & Morton, D. M., 1969. Eclogite inclusions in kimberlite pipes at Garnet Ridge, northeastern Arizona. *American Mineralogist*, **54,** 267–285.
Will, T., Okrusch, M., Schmädicke, E. & Chen, G., 1998. Phase relations in the greenschist-blueschist-amphibolite-eclogite facies in the system Na_2O-CaO-FeO-MgO-Al_2O_3-SiO_2-H_2O (NCFMASH), with application to metamorphic rocks from Samos, Greece. *Contributions to Mineralogy and Petrology*, **132,** 85–102.
Will, T. M. & Powell, R., 1992. Activity-composition relationships in multicomponent amphiboles: an application of Darken's quadratic formalism. *American Mineralogist*, **77,** 954–966.

Received 19 July 2002; revision accepted 14 June 2003.

APPENDIX: MIXING MODELS FOR SOLID SOLUTION PHASES

Lawsonite activity has been taken as unity, because lawsonite analyses do not depart significantly from the ideal composition (e.g. Deer *et al*., 1986). Significant departures from the ideal composition are rarely described, due to substitutions by Cr (Mével & Kiénast, 1980; Sherlock & Okay, 1999) and Sr (Miyajima *et al*., 1999). With the exception of glaucophane, models are taken from Holland & Powell (1998). Nonideality parameters are from Holland & Powell (1998) and the THERMOCALC documentation (Powell & Holland, 2002).

Garnet

variables: x(g) = Fe/(Fe + Mg); z(g) = Ca/(Fe + Mg + Ca)
structural formulae of end-members:
almandine (alm): $Fe_3Al_2Si_3O_8$
pyrope (py): $Mg_3Al_2Si_3O_8$
grossular (gr): $Ca_3Al_2Si_3O_8$
site fractions: $X^{M}_{Fe} = x(1 - z)$; $X^{M}_{Mg} = (1 - x)(1 - z)$; $X^{M}_{Ca} = z$
proportions: p(alm) = x(1 − z); p(py) = (1 − x)(1 − z); p(gr) = z
nonideality: symmetric formalism; w(alm, py) = 2.5 kJ, w(alm, gr) = 0 kJ, w(py, gr) = 33 kJ

Chlorite

variables: x(chl) = bulk Fe/(Fe + Mg); y(chl) = Al (oct)/2 = X^{T2}_{Al}; Q(chl) = $(X^{M4}_{Al} - X^{M1}_{Al})/2$
structural formulae of end-members:
Al-free chlorite (afchl): $Mg_4MgMg[Si_2]Si_2O_{10}(OH)_4$
clinochlore (clin): $Mg_4MgAl[SiAl]Si_2O_{10}(OH)_4$
amesite (ames): $Mg_4AlAl[Al_2]Si_2O_{10}(OH)_4$
daphnite (daph): $Fe_4FeAl[SiAl]Si_2O_{10}(OH)_4$
site fractions: $X^{M23}_{Fe} = x$; $X^{M23}_{Mg} = 1 - x$; $X^{M1}_{Al} = y - Q$; $X^{M1}_{Fe} = x(1 - y + Q)$; $X^{M1}_{Mg} = (1 - x)(1 - y + Q)$; $X^{M4}_{Al} = y + Q$; $X^{M4}_{Mg} = (1 - x)(1 - y - Q)$; $X^{T2}_{Al} = y$; $X^{T2}_{Si} = 1 - y$
proportions: p(afchl) = 1 − y − Q; p(clin) = 2Q − 2x(3 − y)/5; p(ames) = y − Q; p(daph) = 2x(3 − y)/5
nonideality: symmetric formalism; w(afchl, clin) = 18 kJ; w(afchl, ames) = 20 kJ; w(afchl, daph) = 14.5 kJ; w(clin, ames) = 18 kJ; w(clin, daph) = 2.5 kJ; w(ames, daph) = 13.5 kJ

Glaucophane

variables: n(gln) = bulk Na/(Na + Ca); x(gln) = X^{M13}_{Fe}
structural formulae of end-members:
glaucophane (gl): $Na_2Mg_3Al_2Si_4Si_4O_{22}(OH)_2$
tremolite (tr): $Ca_2Mg_3Mg_2Si_4Si_4O_{22}(OH)_2$
ferroactinolite (fact): $Ca_2Fe_3Fe_2Si_4Si_4O_{22}(OH)_2$
site fractions: $X^{M4}_{Na} = n$; $X^{M4}_{Ca} = 1 - n$; $X^{M13}_{Fe} = x$; $X^{M13}_{Mg} = 1 - x$; $X^{M2}_{Al} = n$; $X^{M2}_{Fe} = x(1 - n)$; $X^{M2}_{Mg} = (1 - x)(1 - n)$
proportions: p(gl) = n; p(fact) = x(5 − 2n)/5; p(tr) = 1− n − [x(5 − 2n)/5]
nonideality: DQF: $I^{gln}_{tr} = 45$ kJ (Will & Powell, 1992); $I^{gln}_{fact} = 35$ kJ (Carson *et al*., 1999)

Epidote

variables: x1(ep) = X^{M1}_{Fe}; x3(ep) = X^{M3}_{Fe}
structural formulae of end-members:
clinozoisite (cz): $Ca_2AlAlAlSi_3O_{12}(OH)$
epidote (ep): $Ca_2AlAlFeSi_3O_{12}(OH)$
Fe-epidote (fep): $Ca_2FeAlFeSi_3O_{12}(OH)$
site fractions: $X^{M1}_{Fe} = x1$; $X^{M1}_{Al} = 1 - x1$; $X^{M3}_{Fe} = x3$; $X^{M3}_{Al} = 1 - x3$
proportions: p(cz) = 1 − x3; p(ep) = x3 − x1; p(fep) = x1
nonideality: symmetric formalism; w(cz, ep) = 0 kJ, w(cz, fep) = 15.4 kJ; w(ep, fep) = 3 kJ